Journal of Ideas in Health

e ISSN: 2645-9248 Journal homepage: www.jidhealth.com Open Access

Original Article

# Experimental inoculation of the Botox perineurally of facial nerve and followed by histological assessment for its effect on the zygomatic bone of rabbits

Ali Khudheyer Obayes[1], Sameeah Mejbel Hamad[2*], Huda Ayad Hameed[3]

## Abstract

**Background:** Botox, derived from the toxin produced by Clostridium botulinum, is an attenuated toxin employed as a treatment for cervical dystonia, overactive bladder, strabismus, cerebral palsy, and non-surgical cosmetic procedures. This study aimed to explore the impact of injecting Botox around the facial nerve on the left side of rabbits, specifically focusing on the histological changes in the zygomatic bone.

**Methods:** Twenty-five adult rabbits of a local breed, weighing 1500-1800 gm and of both sexes, underwent a 15-day acclimation period prior to the experiment. The rabbits were randomly assigned to four groups (1st, 2nd, 3rd, and 4th). A singular intramuscular injection of Botox at a dose of 3.5 U/kg was administered to the left facial muscles. The rabbits in each group were then sacrificed at distinct time points after injection: day 10, day 15, day 30, and day 45. All rabbits survived until the end of the experiment, at which point they were euthanized with chloroform. Post-euthanasia, the rabbits' facial zygomatic bones were dissected and subjected to histological assessment.

**Results:** The results indicated notable changes in the zygomatic bone, including prominent vacuoles within the bony matrix, cracks with cellular debris, limited osteocytes, and collagen bundles resembling woven bone. Additionally, in the day 30 group (T3), irregular bone borders and atrophied osteogenic cells were observed, while the day 45 group (T4) exhibited necrotic areas and bone fragments within the bone matrix.

**Conclusion:** In conclusion, Botox, derived from Clostridium botulinum, serves various medical purposes. The study focused on injecting Botox around rabbits' facial nerves to assess its impact on zygomatic bones histologically. Following a controlled injection and specific time intervals, the examined bone samples exhibited distinct changes, providing insights into Botox's effects on bone morphology.

**Keywords:** Botox, Zygomatic bone of Rabbit, Facial Nerve, Iraq

## Background

Botulinum toxin type A (BoNTA) stands as a notably potent variant among a family of neurotoxins generated by the anaerobic bacterium Clostridium botulinum. Its profound impact stems from its capacity to impede the release of acetylcholine from motor neurons, causing a reversible paralysis of skeletal muscles that endures for approximately 4 to 6 months in humans [1].

Although complications linked to injecting BoNTA into the masseter muscle, like transient alterations in bite force, have been documented [2], the intricate interplay between muscles and bones and its potential influence on bone homeostasis remains an area with relatively scant exploration. While the consequences of BoNTA administration on muscle function and degradation have been studied in depth, the secondary implications for bone health have received comparatively less attention. The musculoskeletal framework orchestrates a nuanced equilibrium between muscles and bones, where a sophisticated interplay of biomechanical interactions—ranging from force generation to tension—and intricate biochemical

*Correspondence: med.badeaa.thamir@uoanbar.edu.iq
[2]Department of Anatomy, Faculty of Medicine, Anbar University, Anbar, Iraq

A full list of author information is available at the end of the article

signaling govern the harmony between these two tissues [3]. This dynamic interrelationship involves not only mechanical forces but also a network of molecular cues that are released by muscles, contributing to the delicate balance of bone homeostasis, and reciprocally, bones also influence muscle function. However, the extent to which BoNTA might disrupt this complex interplay between muscles and bones, leading to potential effects on bone health, remains a realm deserving of deeper investigation. In a realm where muscle degradation has demonstrated correlations with bone loss, particularly in individuals with spinal cord injuries [4], delving into the broader implications of BoNTA injections on bone homeostasis could offer valuable insights. In essence, the multifaceted interaction between these two vital tissues could hold clues to understanding not only the therapeutic potentials of BoNTA but also its less-explored effects on the intricate balance of the musculoskeletal system. The intricate connection between muscle function and bone stability operates on both biomechanical and biochemical planes [5]. Bone, a specialized mineralized connective tissue, undergoes a continuous cycle of remodeling characterized by alternating phases of bone formation and resorption. This dynamic process holds the key to repairing and restoring the structure and function of compromised bone tissue, underscoring its remarkable regenerative potential [6]. The interplay between bone formation and resorption cells is pivotal, working in harmony to rejuvenate and maintain bone tissue integrity. This orchestration assumes paramount importance in the healing process, contributing to the restoration of bone's strength and functionality [6]. Moreover, the complexity of bone extends to its rich innervation and vascularization, accompanied by specialized coverings like the periosteum on its outer surface and the endosteum, which interfaces directly with the bone marrow, within [7-10]. The saga continues in the realm of skeletal muscles, where the consequences of denervation have been extensively studied [8-11]. The intricate relationship between muscles and bone health takes center stage when considering conditions in which chronic disruptions in muscle function give rise to a cascade of pathologies [12]. This underscores the integral role that muscles play in safeguarding bone health, revealing a poignant connection that echoes throughout the spectrum of musculoskeletal well-being. Given that muscles constitute the primary force transmitters to the skeletal framework [13], the bones in paralyzed limbs confront a significant deficit in a pivotal stimulus that preserves bone density. Post-spinal cord injury (SCI) osteoporosis emerges through a complex interplay of factors; nevertheless, the reduction in mechanical stimuli to bones stands out as a formidable contributor to the erosion of bone mineral content [14,15]. On the lowest activity rung, when weight-bearing and muscular engagement dwindle or halt post-SCI, the absence of mechanical strain disrupts the equilibrium between osteoclastic and osteoblastic actions. This disparity triggers an acceleration in bone resorption over bone formation, culminating in the emergence of neurogenic osteoporosis. Various animal models, encompassing both small and large species, have been harnessed to dissect the intricacies of bone loss due to disuse. These models encompass diverse approaches such as tendotomy [16], limb immobilization through casting [17], suspension of the hind limbs [18,19], and disruption of nerve function [20-22]. The theoretical foundation introduced by Moss through the functional matrix theory underlines that non-bone tissues exert a regulatory influence on bone growth, particularly evident in facial development. When translated to musculoskeletal dynamics, muscle weakness significantly impairs the trajectory of bone growth and maturation [23]. In essence, the muscle-bone partnership's indispensability becomes apparent as it pertains to the mechanical balance governing bone density and health. In scenarios such as SCI where muscle function wanes, the repercussions cascade through the skeletal structure, emphasizing the pivotal role of muscles in shaping bone health and development. The aim of present study was to reveal histological alteration in zygomatic bone in rabbit induced by paralyzed facial nerve.

## Methods

### Study design and setting

An experimental investigation was conducted within the surgical laboratory of Tikrit University's College of Veterinary Medicine, spanning from March 2023 to June 2023.

### Animals

The experimental cohort consisted of twenty-five adult rabbits of a local breed, encompassing both genders, and with weights ranging from 1500 to 1800 grams. These rabbits, aged between 11 and 13 months, were the subjects of the study. Prior to the commencement of the experiment, the rabbits were acclimated to a controlled environment within an air-conditioned room, maintaining temperatures between 21-25°C. A daily photoperiod of 12 hours was upheld. To ensure the rabbits' well-being, they were granted unhindered access to both food and water before the initiation of the study.

### Experimental Design

The rabbits were then randomly allocated to five distinct groups, with each group comprising five rabbits. Throughout the duration of the experiment, the rabbits were housed in steel cages, each measuring 1.250 meters in length, 0.5 meters in width, and 0.5 meters in height. Stringent care protocols were employed to prevent undue stress on the rabbits, and the cages were meticulously cleaned on a weekly basis. Before embarking on the actual experimental procedures, a preparatory period of at least 15 days was provided to the rabbits to adapt to their surroundings and conditions. This period of adjustment ensured that the rabbits were acclimated and prepared for the subsequent phases of the study. The study was structured with the intention of clarifying the impact of facial nerve paralysis on the zygomatic bone in rabbits. The rabbits were subjected to a facial injection of BTXA at a dosage of 3.5 U/kg [24]. The experimental procedure encompassed four distinct groups, each of which underwent perineural inoculation of Botox. For this purpose, a 25-gauge needle measuring 1.0 cm in length was utilized to administer the requisite amount of Botox. The animals were subjected to distinct observation periods, outlined as follows: In the first group (Group 1), comprising five rabbits, the animals were sacrificed ten days post-inoculation. Similarly, in the second group (Group 2), the rabbits were sacrificed after fifteen days of inoculation. The third group (Group 3) underwent sacrifice after a period of thirty days following

inoculation. Lastly, the fourth group (Group 4) was subjected to sacrifice after a period of forty-five days post-inoculation.

### Specimen Extraction

All the animals were carefully monitored until the predetermined endpoints of the study, after which they were humanely euthanized through inhalation of a concentrated dose of chloroform within a sealed glass enclosure. Following euthanasia, the animals were subjected to dissection, and samples were collected from both the experimental and control groups. These specimens were immersed in a 10% neutral buffer formalin solution for 48 hours to facilitate fixation. To prepare the specimens for analysis, a series of meticulous steps were undertaken. The samples underwent decalcification in a sequence involving acetic acid and subsequently nitric acid, each spanning a week. After this process, the bone tissue samples from the rabbit's zygomatic bone were meticulously readied for histological analysis. Gradually increasing concentrations of alcohol (70%, 80%, 90%, and 100%) were used to immerse the samples. This was followed by clearing with xylene, after which the samples were embedded in paraffin wax at a temperature of 60°C. The prepared samples were then blocked and finely sectioned to a thickness of 5 µm using a rotary microtome. Once the sections were appropriately prepared, they underwent Hematoxylin and Eosin staining. These stained tissue sections were carefully mounted onto slides using D.P.X and sealed with cover slides [12,25]. The next stage involved a thorough examination of the slides using a light microscope, with the resulting observations documented through photography facilitated by a dedicated camera setup. This meticulous procedure allowed for the detailed analysis of the histological characteristics and changes within the specimens.

## Results

### T1 group

The composition of the bony matrix revealed the presence of osteocytes housed within lacunae. Interestingly, the matrix exhibited conspicuous vacuoles, accommodating cellular components within their confines. These vacuoles also contained necrotic cells. This depiction is visually presented in Figure 1.

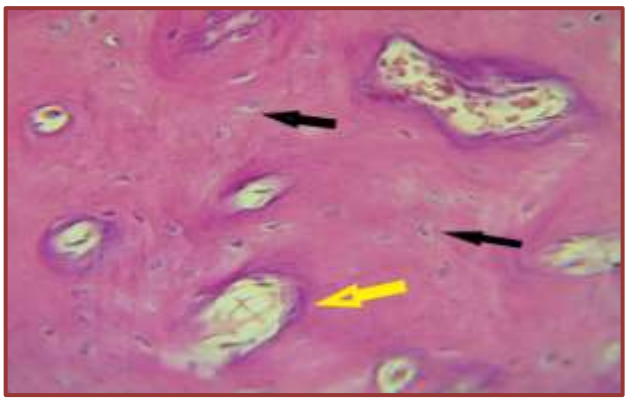

**Figure 1:** Rabbit zygomatic bone T1, Bone matrix, great vacuoles and cellular debris (Yellow arrow) osteocyte in lacunae (Black), (H&E X 40).

As the bony matrix extended longitudinally, it encountered a proliferation of lacunae populated with osteocytes. Remarkably, discernible cracks traversed the matrix, accompanied by fragments of detached bone tissue. These fragments bore evidence of residual cellular debris. This visual representation is captured in Figure 2.

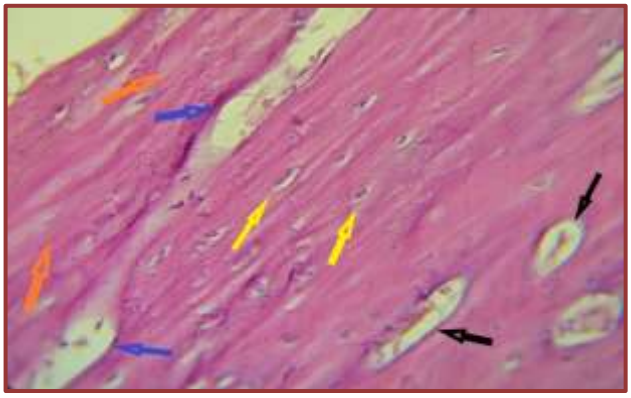

**Figure 2:** Rabbit zygomatic bone T1, Bony matrix osteocytes in lacunae (Yellow arrow), great vacuoles for haversian canals (Black arrow), crack with cellular debris (Blue arrow), detached collar bone (orange arrow), (H&E X 40).

A detailed examination of the bony matrix unveiled a density of osteocytes ensconced within lacunae. The nuclei of these cells stood out prominently. Along the borders of the bone, distinct depressions could be observed. Here, a sparse presence of osteoblasts was evident, and a delicate connective tissue fibrous coat was discernible. Adjacent to the bone tissue, there existed scattered skeletal muscle fibers. This visual representation is captured in Figure 3.

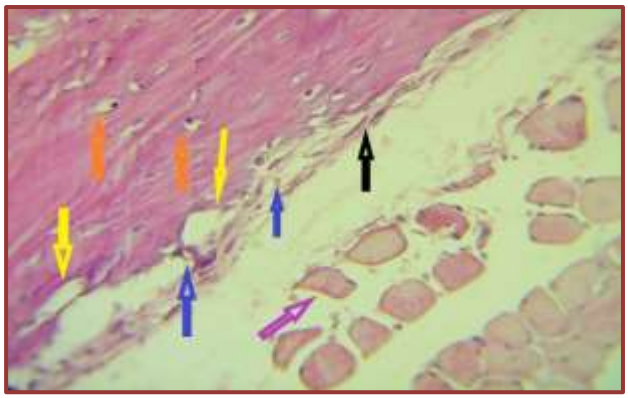

**Figure 3:** Rabbit zygomatic boneT1group, lacunae with prominent nuclei (Brown arrow), irregular bone border (Yellow arrow), few osteoblasts (Blue arrow), delicate fibrous tissue (Black arrow), scattered skeletal muscles (Purple arrow), (H&E X 40).

### T2 group

The bony matrix exhibited a scarcity of osteocytes, and within this matrix, collagen bundles mimicking the appearance of woven bone were discernible. A few cavities harboring cellular debris became evident, while the bone's borders displayed an irregular profile, juxtaposed with various types of marrow cells. This visual representation is captured in Figure 4. Within the bone tissue, a robust level of ossification was observable. The matrix housed osteocytes, while sizable cavities still persisted, encapsulating limited marrow cells. Interestingly, the arrangement of bony lamellae did not conform to a concentric pattern. This is illustrated in Figure 5. The bony matrix showcased the presence of Haversian canals aligned

longitudinally, alongside Volkmann's canals oriented horizontally with respect to the bone's axis. Notably, these canals accommodated red blood cells, indicating their function as conduits for blood vessels. The periosteum, comprising a fibrous coat, appeared detached from the bone's outer surface. Importantly, no evidence of osteogenic or osteoblastic presence was observed.

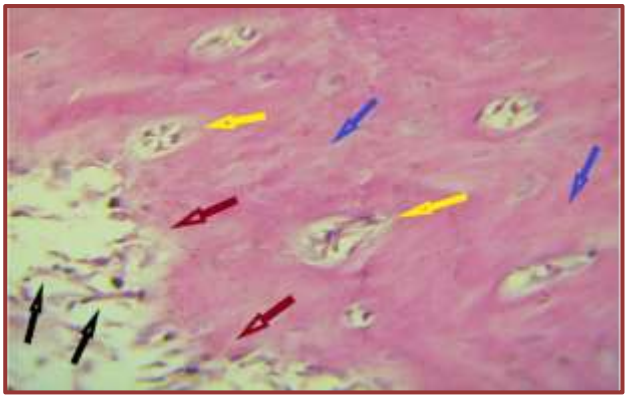

**Figure 4:** Rabbit zygomatic bone T1 group, woven bone with collagen bundles in matrix (Blue arrow), cavities with RBCs (Yellow arrow), irregular bone border (Brown arrow), bone marrow cells (Black arrow), (H&E X 40).

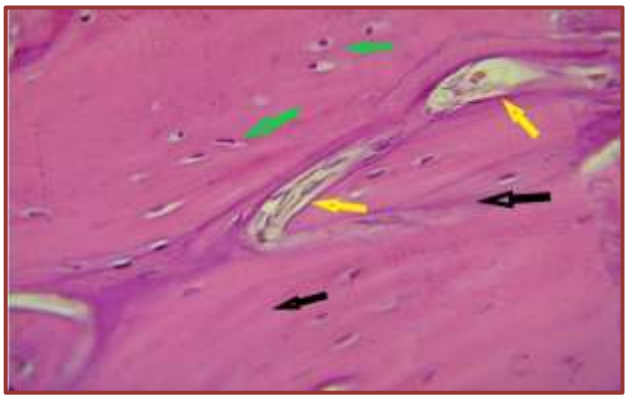

**Figure 5:** Rabbit zygomatic bone group T2, irregular bony lamellae (Black arrow), bony sinuses with marrow cells (Yellow arrow), osteocytes with lacunae (Green arrow), (H&E X 40).

Refer to Figure 6 for visual context. The bony tissue presented multiple lacunae housing osteocytes within. These osteocytes were distributed randomly across the matrix. The bone's periphery featured a collar formation, encircled by strands of collagen bundles.

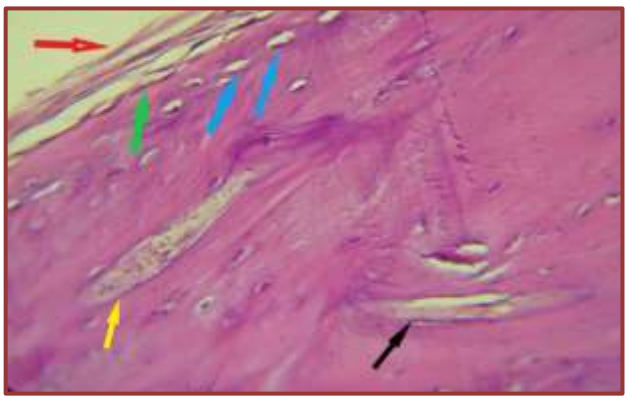

**Figure 6:** Rabbit zygomatic bone group T2, harversian canal with RBCs (Yellow arrow), Volkmann with micro blood vessels (Black arrow), lacunae without osteocytes (Blue arrow), fibrous coat of periosteum (Red arrow), no indication for osteoblast or osteogenic cells (Green arrow), (H&E X 40).

This depiction is encapsulated in Figure 7. In another view, the bony tissue displayed osteocytes within lacunae, and conspicuous dark patches indicating remnants of hyaline cartilage were evident. The border of the bone was noted to contain hypertrophic osteogenic cells. See Figure 8 for visual insight.

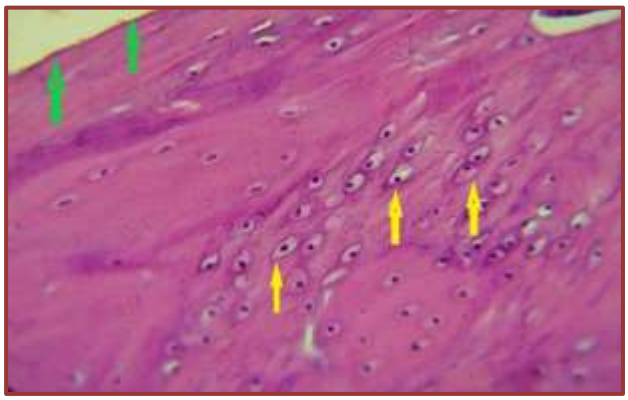

**Figure 7:** Rabbit zygomatic bone group T2, bony matrix with randomly distributed of osteocytes in lacunae (Yellow arrow), periosteum with strands of collagen fibers (Green arrow), (H&E X 40).

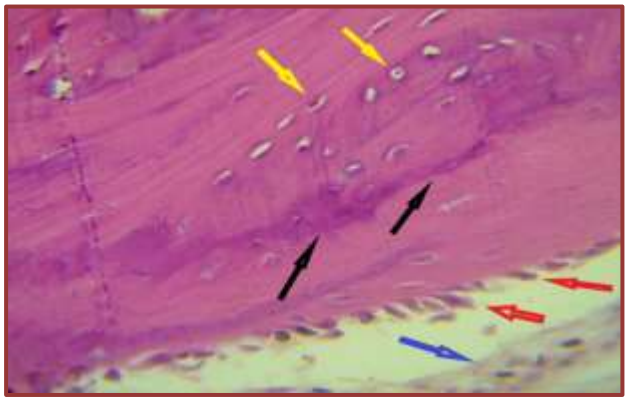

**Figure 8:** Rabbit zygomatic bone group T2, osteocytes in lacunae (Yellow arrow), remnant of hyaline cartilage (Black arrow), hypertrophy of osteoblasts (Red arrow), fibrous coat of periosteum (Blue arrow), (H&E X 40).

### T3 group

Within the bony tissue, numerous marrow cavities of varying sizes were evident. These could be considered as potential future Haversian and Volkmann's canals. Additionally, osteocytes occupied lacunae in the matrix. Along the bone's periphery, the periosteum was absent, while clusters of osteogenic and osteoblast cells were observed. Please refer to Figure 9 for visual reference. Substantial marrow cavities were interspersed within the bony matrix. These cavities contained cellular debris and red blood cells, signifying their eventual transformation into future Haversian canals. The periosteum featured an outer layer composed of a fibrous coat primarily constituted by collagen bundles, alongside fibroblasts. The inner layer comprised osteogenic cells, distributed in a scattered pattern along the bone's border. This visualization is depicted in Figure 10. The outer boundary of the bone exhibited irregularities, with prominent cavities filled with masses of necrotic cells. The osteogenic cells were characterized by atrophy, adopting a spindle-like morphology. Within the bony matrix, small osteocytes were found within lacunae. This representation can be observed in Figure 11.

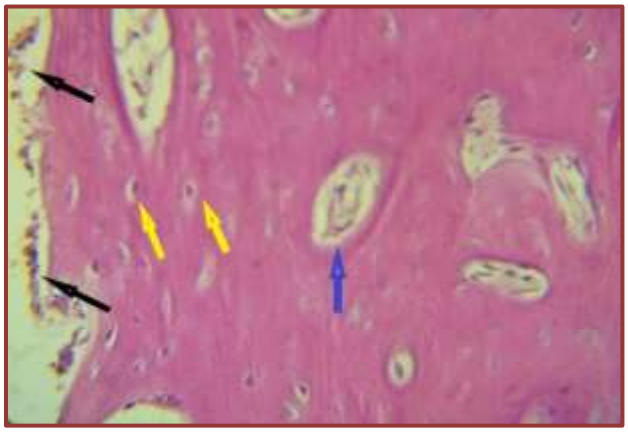

**Figure 9:** Rabbit zygomatic bone group T3, bony matrix with marrow cavities (Blue arrow), osteocytes within lacunae (Yellow arrow), clump of osteogenic cells (Black arrow), (H&E X 40).

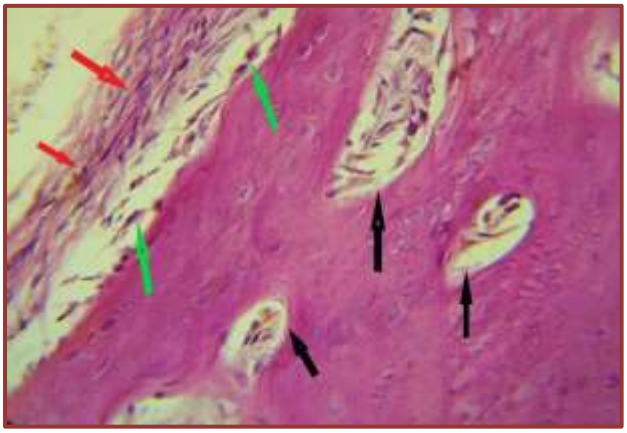

**Figure 10:** Rabbit zygomatic bone group T3, great marrow cavities with RBCs with cellular debris (Black arrow), fibrous collagenous layer of periosteum (Red arrow), scattered osteogenic cells (Green arrow), (H&E X 40).

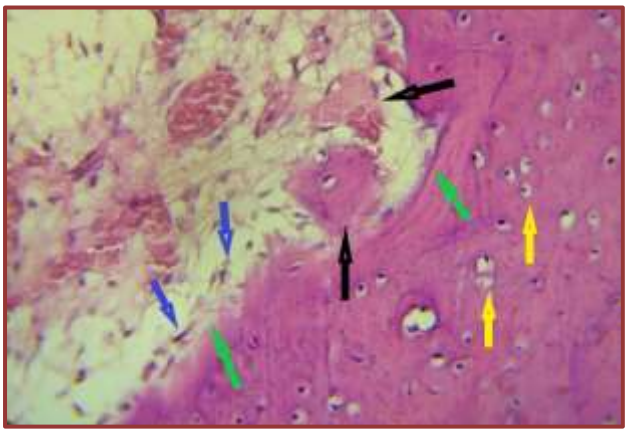

**Figure 11:** Rabbit zygomatic bone group T3, bone tissue irregular border of bone (Green arrow), atrophied osteogenic cells (Blue arrow), necrotic cells of bone tissue (Black arrow), lacunae with small osteocytes (Yellow arrow), (H&E X 40).

Notably, the bony tissue retained traces of cartilage. The osteocytes within displayed signs of atrophy, and their lacunae appeared distorted. The outer border of the bone exhibited an absence of osteogenic cells, while the fibrous coat appeared detached from the bone surface. Please refer to Figure 12 for visual insight.

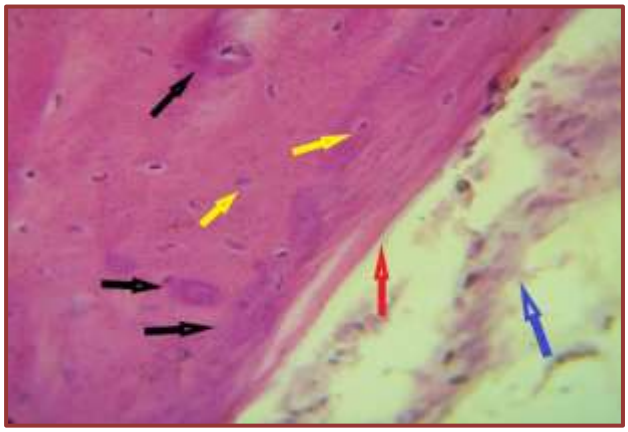

**Figure 12:** Rabbit zygomatic bone group T3, bone tissue, atrophied osteocytes (Yellow arrow), remnant of cartilage (Black arrow) absence of osteogenic cells (Red arrow), detachment of fibrous layer of periosteum (Blue arrow), (H&E X 40).

### T4 group

The composition of the bony matrix unveiled a multitude of sizable cavities and sinuses. Within this matrix, osteocytes were situated within lacunae. Notably, one border of the bone featured the presence of osteoblasts, while the other border was characterized by strands of collagen fibers. Please refer to Figure 13 for visual context. The matrix of the bone exhibited necrotic regions occupied by degenerated osteocytes. Detached fragments of bone were also visible. In a distinct pattern, osteoblasts formed rows along the bone's border. Conversely, the opposing border appeared irregular and displayed a scarcity of osteoblasts or osteogenic cells, apart from the delicate connective tissue component. This depiction is presented in Figure 14. The bone tissue was notably well-ossified, with bony lamellae embedded within. These lamellae contained lacunae housing osteocytes. One of the bone's borders displayed signs of atrophy, while the adjacent border presented osteoblasts. A unique feature was the presence of tongue-like projections of accessory bone along this border, partially detached from the cortical bone. Refer to Figure 15 for visual insight. A closer examination of the bony matrix revealed the existence of sizable lacunae housing osteocytes. The matrix was adorned with collagen bundles resembling the structure of woven bone. Along the bone's border, a bundle of collagen fibers could be observed, devoid of any periosteum. Additionally, necrotic cells were discernible at the bone's periphery. This is illustrated in Figure 16. The arrangement of bony lamellae within the matrix was distinctly evident, associated with the presence of osteocytes within their lacunae. One border of the bone showcased substantial vacuoles containing cellular elements, in the absence of any periosteum. This depiction can be observed in Figure 17. As the view transitions to the peripheral border of the bone, a pattern of cracks becomes apparent, accompanied by the presence of numerous red blood cells. Meanwhile, the larger vacuoles within the bony matrix persisted, interspersed with smaller ones alongside lacunae containing osteocytes. The Haversian canals were revealed to contain blood vessels. This visual representation is encapsulated in Figure 18. The bone tissue revealed remnants of necrotic material, characterized by dark regions. Notably, the presence of substantial cavities was evident, accompanied by sparse cellular components. Within the matrix, a limited number of osteocytes occupied lacunae,

with their nuclei infrequently discernible. This depiction is presented in Figure 19. The peripheral border of the bone tissue exhibited irregularities, characterized by prominent voids filled with necrotic cells. Additionally, a small number of atrophied osteoblasts were observable along the bone's border. Furthermore, the bony matrix contained a sparse number of cavities that potentially indicated future Haversian canals. These cavities were encircled by lamellae forming the bone's structure, closely associated with osteocytes within their lacunae. Please refer to Figure 20 for visual insight.

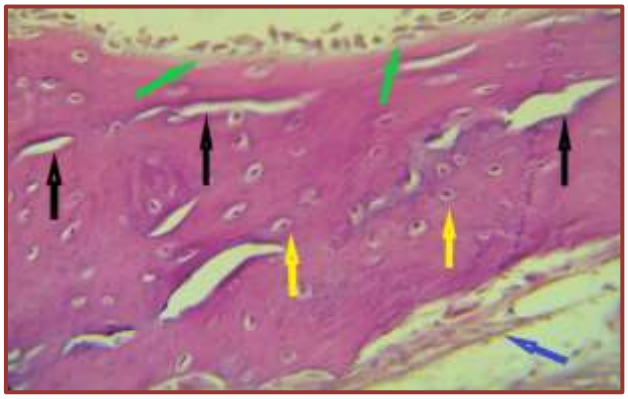

**Figure 13:** Rabbit zygomatic bone T4 group, bone tissue, great cavities and sinuses in bone matrix (Black arrow), osteocytes on its lacunae (Yellow arrow), osteogenic and osteoblasts cells (Green arrow), strands of collagen fibers (Blue arrow), (H&E X 40).

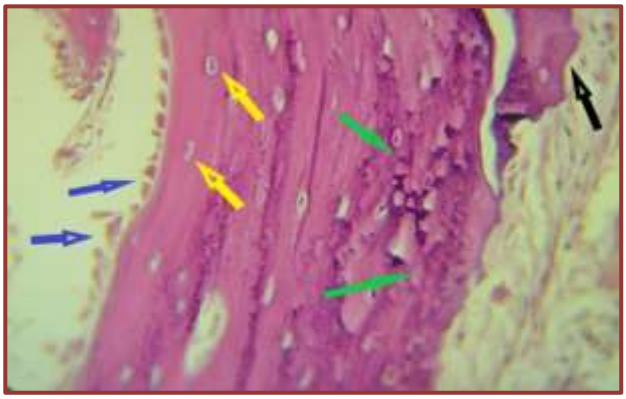

**Figure 14:** Rabbit zygomatic bone T4 group, bone tissue, necrotic area with osteocytes and lacunae (Green arrow), degenerated and detached bony mass (Black arrow), osteoblasts (Blue arrow), osteocytes in its lacunae (Yellow arrow), (H&E X 40).

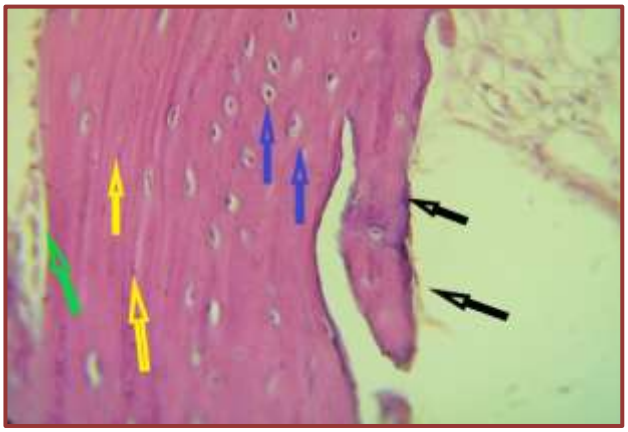

**Figure 15:** Rabbit zygomatic bone T4 group, bone tissue, bony lamellae (Yellow arrow), osteocytes and lacunae (Blue arrow), atrophied osteoblasts (Green arrow), accessory bony tissue (tongue like projection) (Black arrow), (H&E X 40).

## Discussion

The utilization of BTX-A for both therapeutic and aesthetic purposes has gained widespread endorsement among medical professionals due to its established safety and effectiveness [26]. Within this context, the current study was meticulously designed to delve into the impact of Botox on the zygomatic bone within the facial region of rabbits. The histological scrutiny conducted in this study illuminated intriguing findings. The bony matrix showcased the presence of collagen bundles, bearing a striking resemblance to the appearance of woven bone. Noteworthy were the small cavities harboring cellular debris, coupled with the irregular borders of the bone adjacent to the neighboring bone marrow. The presence of black patches, reminiscent of remnants of hyaline cartilage, was a distinctive observation, along with the detection of hypertrophic osteogenic cells at the bone's border [27]. Interestingly, findings from Ali et al.'s research in 2018 are in alignment with our observations. They highlighted the presence of multiple scattered areas in the bone matrix exhibiting less acidophilic staining. These areas were notably evident on both the endosteal surface and within the bone matrix itself [28]. It is plausible to interpret this as a compensatory mechanism aimed at fortifying bone strength in the face of potential bone loss [29]. The findings from the T4 group unveiled a noteworthy escalation in deficits concomitant with the prolonged period of facial nerve paralysis. Intriguingly, remnants of cartilage embedded within the bone matrix were apparent. Atrophied osteocytes displayed an ill-defined lacunae appearance. Additionally, the bony matrix exhibited an array of significant cavities and sinuses, alongside the presence of osteocytes within their lacunae. A separate avenue of inquiry involved the injection of BTXA in fractured hind limbs of rats. Within this framework, fibrous calluses in the fractured area underwent a continuous transformation into woven bone. This intriguing observation could possibly be attributed to the reduced axial stress loading stemming from quadriceps atrophy, a consequence of the facial nerve paralysis [30]. In the context of the T4 group, the microscopic examination brought to light several compelling features. Notably, substantial vacuoles within the bone's border were teeming with necrotic cells, accompanied by atrophied periosteum. Dark regions denoted remnants of necrotic tissue. The presence of scattered irregular bone resorption cavities was evident, housing numerous osteoclasts. A particularly remarkable observation was the presence of a conspicuous vacant lacuna. In a substantial proportion of sections, the hormonal influence of parathyroid hormone (PTH) was hypothesized to contribute to the speculated osteocyte lysis, thereby underscoring its impact [31,32]. Takata and Yasui [33] proposed a notion suggesting that the disuse of BTX was linked to an imbalance in bone remodeling. This imbalance is marked by an increase in bone resorption alongside a decrease in bone formation. Dutra et al. [34], in their study, postulated that injecting BTX into the masseter muscle leads to reduced mineralization and matrix deposition. This is accompanied by a decrease in osteoclastic activity. The mechanism of BTX action involves the inhibition of acetylcholine (ACH) release in response to nerve impulses. Consequently, the level of ACH can potentially contribute to bone preservation, thus influencing the observed BTX-induced osteoporotic changes [35]. Ashley et al. [36] shed light on vascular changes stemming from denervated muscles, which include the loss of contractile activity and a diminished muscle vascular pump. Simultaneously, the disruption of vasoconstrictor nerve fibers could lead to a loss of vascular tone, thereby impacting the vascular blood flow in both muscle and bone tissues.

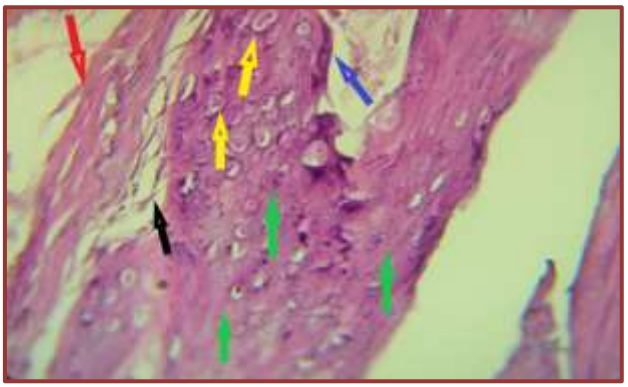

**Figure 16:** Rabbet zygomatic bone T4 group, bone tissue, intermingle with collagen bundles (Green arrow), necrotic cells (Blue arrow), large lacunae with osteocytes (Yellow arrow), collagen bundles with periosteum (Red arrow), atrophied or osteogenic cells (Black arrow), (H&E X 40).

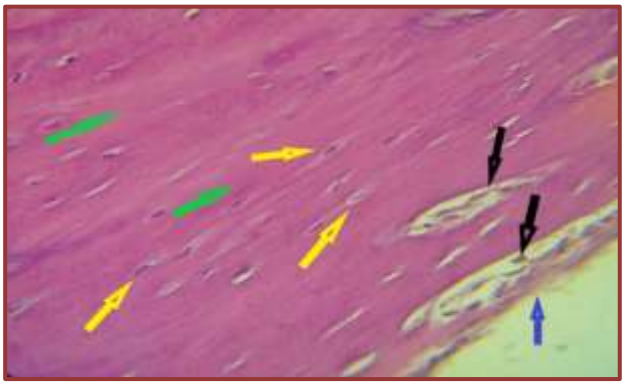

**Figure 17:** Rabbit zygomatic bone T4 group bone tissue, bony lamellae (Green arrow), small lacunae with atrophied osteocytes (Yellow arrow), great vacuoles with cellular elements (Black arrow), periosteum was absent (Blue arrow), (H&E X 40).

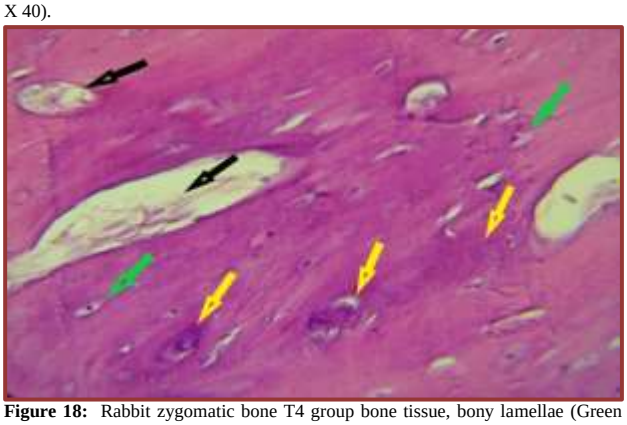

**Figure 18:** Rabbit zygomatic bone T4 group bone tissue, bony lamellae (Green arrow), partial detachment of bone (Red arrow), cellular elements (Black arrow), lacunae with osteocytes (Yellow arrow), haversian canal with osteocytes with micro- blood vessels (Blue arrow), (H&E X 40).

## Conclusion

In summary, the current investigation elucidated that a solitary administration of Botox resulted in distinctive effects. Notably, it prompted the emergence of substantial vacuoles containing cellular components within osteocytes. Cracks manifested within the bony matrix, accompanied by cellular debris. The presence of sparse osteocytes contrasted with the appearance of collagen bundles resembling woven bone. An irregular outer bone border presented itself, featuring atrophied osteogenic cells. Moreover, necrotic regions within the bone matrix, along with detached bone fragments, were evident. These collective observations suggest a toxic impact of Botox on the examined facial bone.

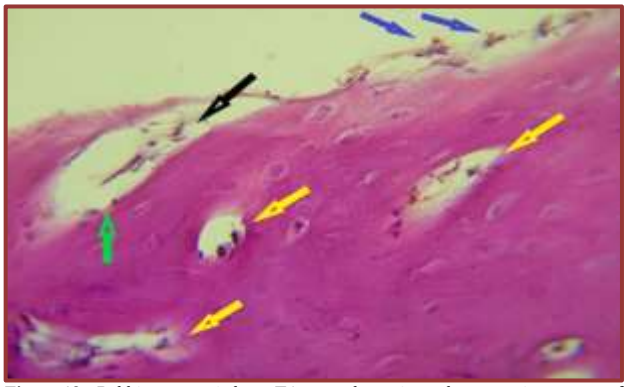

**Figure 19:** Rabbit zygomatic bone T4 group, bone tissue, bony matrix remnant of necrotic tissue (Yellow arrow), great cavities with a few cellular elements (Black arrow), lacunae with osteocytes and ill- defined nuclei (Green arrow), (H&E X 40).

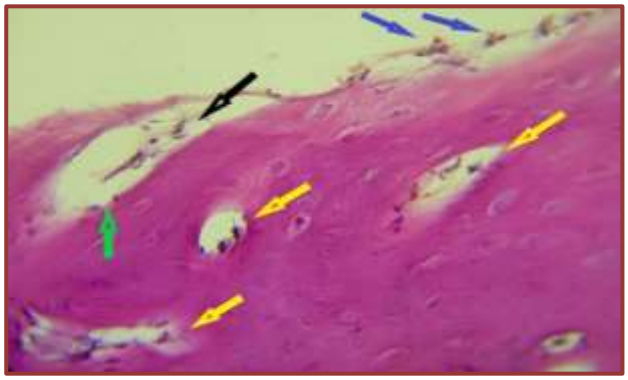

**Figure 20:** Rabbit zygomatic bone T4 group, bone tissue, irregular bony border with tunnel like furrow (Green arrow), necrotic cells (Black arrow), atrophied osteoblasts (Blue arrow), sinuses of future canals (Yellow arrow), (H&E X 40).

### Abbreviation

BoNTA: Botulinum Toxin Type A; SCI: Spinal Cord Injury; ACH: Acetylcholine; PTH: Parathyroid Hormone

### Declaration

### Acknowledgment

None.

### Funding

The author received no financial support for the research, authorship, and/or publication of this article.

### Availability of data and materials

Data will be available by emailing sameeahalgenabi@gmail.com

### Authors' contributions

All authors Ali Khudheyer Obayes (AKY), Sameeah Mejbel Hamad (SMH), and Huda Ayad Hameed (HAH) are equally participated in the concept, design, literature search, data analysis, data acquisition, manuscript writing, editing, and reviewing. All authors have read and approved the final manuscript.

### Ethics approval and consent to participate

The study was conducted in accordance with the ethical principles of the Declaration of Helsinki (2013). The protocol was approved by the Ethics Committee of the Scientific Issues and Postgraduate Studies Unit (PSU), College of Medicine, University of Anbar (Ref: SR/207 at 29-February-2023).

**Consent for publication**
Not applicable

**Competing interest**
The authors declare that they have no competing interests.



**Author Details**
[1]Department. of Pathological Analysis, College of Applied science, University of Samarra, Iraq. [2]Department of Anatomy, Faculty of Medicine, Anbar University, Anbar, Iraq. [3]Department of physiology, pharmacology and biochemistry, College of Veterinary Medicine, Tikrit University.

**Article Info**
Received: 27 June 2023
Accepted: 25 August 2023
Published: 03 September 2023

## References

1. Miller J, Clarkson E. Botulinum Toxin Type A: Review and Its Role in the Dental Office. Dent Clin North Am. 2016;60(2):509-521. DOI: 10.1016/j.cden.2015.11.005.
2. Kim H, Yum K, Lee S, Heo M, Seo K. Effects of botulinum toxin type A on bilateral masseteric hypertrophy evaluated with computed tomographic measurement. Dermatol Surg. 2003; 29:484-489. DOI: 10.1046/j.1524-4725.2003.29120. x.
3. Brotto M, Bonewald L. Bone and muscle: Interactions beyond mechanical. Bone. 2015; 80:109-114. DOI: 10.1016/j.bone.2015.03.014.
4. Warner S, Sanford D, Becker B, Bain S, Srinivasan S, Gross T. Botox induced muscle paralysis rapidly degrades bone. Bone. 2006;38(2):257-264. DOI: 10.1016/j.bone.2005.08.007.
5. Laurent M, Dubois V, Claessens F, Verschueren S, Vanderschueren D, Gielen E, Jardi F. Muscle-bone interactions: From experimental models to the clinic? A critical update. Mol Cell Endocrinol. 2016; 432:14-36. DOI: 10.1016/j.mce.2016.05.010.
6. Vieira A, Repeke C, Junior S, Colavite P, Biguetti C, Oliveira R, Garlet G. Intramembranous bone healing process subsequent to tooth extraction in mice: micro-computed tomography, histomorphometric and molecular characterization. PLoS One. 2015;10(5):e0128021. DOI: 10.1371/journal.pone.0128021.
7. Lai X, Price C, Lu X, Wang L. Imaging and quantifying solute transport across periosteum: Implications for muscle-bone crosstalk. Bone. 2014; 66: 82-89. DOI: 10.1016/j.bone.2014.05.012.
8. Morrison S, Scadden D. The bone marrow niche for haematopoietic stem cells. Nature. 2014; 505: 327-334. DOI: 10.1038/nature12984.
9. Bellido T, Plotkin L, Bruzzaniti A. Bone Cells A2. In Basic and Applied Bone Biology; Allen M.R., Burr D.B., Eds.; Academic Press: San Diego, CA, USA. 2014.
10. Hamad MS. Detection of stem cells in human endometrium: immunohistochemical study. Jidhealth. 2022 May 14;5(2):669-672. doi: 10.47108/jidhealth.vol5.iss2.219.
11. Ehmsen J.T, Hoke A. Cellular and molecular features of neurogenic skeletal muscle atrophy. Exp Neurol. 2020;331:113379. DOI: 10.1016/j.expneurol.2020.113379.
12. Chaudhari A, Chauhan N, Anoop S, Patil S, Chandra R, Lakhkar N. Histological and histomorphometrical evaluation of porous phosphate glass as a bone graft substitute: A pilot study. Journal of Osseointegration. 2022;14(2):88-96. DOI: 10.23805/jo.2022.14.02.02.
13. Lu T, Taylor S, O'Connor J, Walker P. Influence of muscle activity on the forces in the femur: An in vivo study. J Biomech. 1997;30(11-12):1101-1106. DOI: 10.1016/S0021-9290(97)00068-9.
14. Lanyon L. Using functional loading to influence bone mass and architecture: Objectives, mechanisms, and relationship with estrogen of the mechanically adaptive process in bone. Bone. 1996;18(1Suppl):37S-43S. DOI: 10.1016/8756-3282(95)00457-2.
15. Schultheis L. The mechanical control system of bone in weightless spaceflight and in aging. Exp Gerontol. 1991;26(2-3):203-214. DOI: 10.1016/0531-5565(91)90012-7.
16. Shaker J, Fallon M, Goldfarb S, Farber J, Attie M. reduces bone loss after hindlimb tenotomy in rats. J Bone Miner Res. 1989;4:885-890. DOI: 10.1002/jbmr.5650040616.
17. Liu D, Zhao C, Li H, Jiang S, Jiang L, Dai L. Effects of spinal cord injury and hindlimb immobilization on sublesional and supralesional bones in young growing rats. Bone. 2008; 43:119-125. DOI: 10.1016/j.bone.2008.02.010.
18. Barou O, Valentin D, Vico L, Tirode C, Barbier A, Alexandre C, Lafage-Proust MH. High-resolution three-dimensional micro-computed tomography detects bone loss and changes in trabecular architecture early: comparison with DEXA and bone histomorphometry in a rat model of disuse osteoporosis. Invest Radiol. 2002; 37:40-46. DOI: 10.1097/00004424-200201000-00007.
19. Weinre M, Rodan G, Thompson D. Osteopenia in the immobilized rat hind limb is associated with increased bone resorption and decreased bone formation. Bone. 1989; 10:187-194. DOI: 10.1016/8756-3282(89)90042-1.
20. Kingery W, Offley S, Guo T, Davies M, Clark J, Jacobs C. A substance P receptor (NK1) antagonist enhances the widespread osteoporotic effects of sciatic nerve section. Bone. 2003; 33:927-936. DOI: 10.1016/S8756-3282(03)00257-0.
21. Zeng Q, Jee W, Bigornia A, King J, D'Souza S, Ma Y, Wechter WJ. Time responses of cancellous and cortical bones to sciatic neurectomy in growing female rats. Bone. 1996;19:13-21. DOI: 10.1016/8756-3282(95)00502-4.
22. Naser AS, Alberifkani NM. Assessment of anxiolytic-like effects of acute and chronic treatment of flurbiprofen in murine. Jidhealth. 2023 Mar 22;6(1):814-819. doi: 10.47108/jidhealth.vol6.iss1.268.
23. Moss ML, Salentijn L. The primary role of functional matrices in facial growth. Am J Orthod. 1969; 55: 566-577.
24. Fortuna R, Vaz M, Youssef A, Longino D, Herzog W. Changes in contractile properties of muscles receiving

repeat injections of botulinum toxin (Botox). J Biomech. 2011;44(1):39-44. DOI: 10.1016/j.jbiomech.2010.09.030.
25. Yaseen SM, Ali Jadoo SA. Aqueous extract of beetroot against metronidazole toxic influences on glutathione peroxidase activity, spermatogenesis and hematological indices: in vivo study. Ejbps. 2017;4(9):112-115.
26. Suvarna K, Layton C, Bancroft J. Bancroft's theory and practice of histological techniques. Elsevier Health Sciences. 2018. pp79-186.
27. Srivastava S, Kharbanda S, Pal U. Applications of botulinum toxin in dentistry: a comprehensive review. Natl J Maxillofac Surg. 2015;6(2):152-159. DOI: 10.4103/0975-5950.183878.
28. Ali D, Abdelzaher W, Abdel-Hafez S. Evaluation of the rivastigmine role against botulinum toxin-A-induced osteoporosis in albino rats: A biochemical, histological, and immunohistochemical study. Hum Exp Toxicol. 2018;37(12):1323-1335. DOI: 10.1177/0960327118759123.
29. Chen H, Tian X, Liu X. Alfacalcidol-stimulated focal bone formation on the cancellous surface and increased bone formation on the periosteal surface of the lumbar vertebrae of adult female rats. Calcif Tissue Int. 2008; 82:127-136. DOI: 10.1007/s00223-007-9154-0.
30. Hao Y, Ma Y, Wang X, Jin F. Short-term muscle atrophy caused by botulinum toxin-A local injection impairs fracture healing in the rat femur. J Orthop Res. 2012;30(4):574-580. DOI: 10.1002/jor.21553.
31. Tsazawa K, Hoshi K, Kawamoto S, et al. Osteocytic osteolysis observed in rats to which parathyroid hormone was continuously administered. J Bone Miner Metab. 2004;22:524-529. DOI: 10.1007/s00774-004-0524-5.
32. Warner S, Sanford D, Becker B. Botox induced muscle paralysis rapidly degrades bone. Bone. 2006;38(2):257-264. DOI: 10.1016/j.bone.2005.08.007.
33. Takata S, Yasui N. Disuse osteoporosis. J Med Invest. 2001; 48:147-156.
34. Dutra E, Brien H, Kalajzic Z. Cellular and matrix response of the mandibular condylar cartilage to botulinum toxin. PLoS One. 2016;11(10): e0164599. DOI: 10.1371/journal.pone.0164599.
35. Schiavo G, Matteoli M, Montecucco C. Neurotoxins affecting neuroexocytosis. Physiol Rev. 2000; 80:717-766. DOI: 10.1152/physrev.2000.80.2.717.
36. Ashley Z, Sutherland H, Lanmuller H, Russold MF, Unger E, Bijak M, Jarvis JC. Atrophy, but not necrosis, in rabbit skeletal muscle denervated for periods up to one year. Am J Physiol-Cell Physiol. 2007;292(1):C440-C451. DOI: 10.1152/ajpcell.00106.2006.